Theoretical and Experimental Investigation of Interactions between River Flow and Seepage Flow

Article · January 2009

2 authors:

Upaka Rathnayake
Sri Lanka Institute of Information Technology
96 PUBLICATIONS 386 CITATIONS

SEE PROFILE

Norihiro Izumi
Hokkaido University
149 PUBLICATIONS 1,240 CITATIONS

SEE PROFILE

Some of the authors of this publication are also working on these related projects:

Channelization on slopes View project

Impact of climate variability on agriculture View project

Theoretical analysis for the interaction between the river flow and the seepage flow

UPAKA RATHNAYAKE, NORIHIRO IZUMI
Department of Civil Engineering
Hokkaido University
River and Watershed Engineering Laboratory, Graduate School of Engineering, Hokkaido University
JAPAN
upaka@eng.hokudai.ac.jp, nizumi@eng.hokudai.ac.jp

Abstract: Many previous studies have been carried on the interaction between river flow and the seepage flow in the environmental point of view, but these hardly touch on the boundary conditions or the limitations for the interactions. The subsurface layer below the river is known as the hyporheic layer and it is a saturated band of sediment that surrounds river flow and forms a linkage between the river and the aquifer. The large velocity difference between the river flow layer and the seepage flow layer causes the instability of the flows. Due to this flow instability, a reciprocating flow motion is generated between the hyporheic layer and the above.

Linear stability analysis technique is used to understand the stability of the natural flows in rivers as well as the flows occurred in the air by many researchers. In this study a linear stability analysis is carried out to presents the interaction between the river flow and seepage flow. Reynolds averaged Navier-Stokes equations and Brinkman-Forchheimer equations are used in order to formulate the river flow and seepage flow interaction. The open channel flow is analyzed by mixing length turbulent model and Spectral collocation method incorporated with the Chebyshev polynomials are used to perform the numerical solution of the perturbed equations.

Instability diagrams are discussed with several slopes of the layers against the dimensionless particle diameter and wave numbers. It has been noted that the instability occurs even in the range of small dimensionless particle diameter with relatively high wave numbers if there is a seepage layer beneath the flow and the instability region increases with the slope when the wave numbers are at small values.

Key-Words: - river flow, seepage flow, linear stability analysis, perturbations, growth rate contours

1 Introduction

Natural flows like river flow are difficult to be treated as lined cannel flow since the flow is influenced by the seepage flow. Literature shows that there is a great deal of research on the title in the environmental point of view, but few on the mechanism of interaction and the limitations for the interaction.

Hyporheic layer can be defined as an active transition zone between the surface river and ground water, exchanging water, nutrients and organic matter. Up-welling subsurface water supplies river organisms with nutrients while down-welling river water provides dissolved oxygen and organic matter to microbes and invertebrates in the hyporheic zone equations *(Andrew J. Boulton et al 1998, Daniele Tonina et al 2007 and Andrea Butturini et al 2002)*. Some analysis shows that the hyporheic zone is facilitating to exchange at-least 10% of the river water flow *(Kenneth E. Bencala, 2000)*. These transitions are occurred due to the velocity differences in the two distinct flows. Rivers have currents generating turbulence and variable velocities, discharges in contrast the groundwater environments are stable with laminar flow. The difference of the velocities among the two layers is led to the instability at the interface between fast river flow and slow seepage flow.

Therefore it is important to examine the instability between the river and seepage flows to present the limitations of the interactions.

2 Conceptual Model

Figure 1 shows the conceptual model which is used to formulate the both river and the seepage flow. The flow on the permeable layer is assumed to be in the normal flow condition and if this normal flow condition is stable, there is no water exchange between flows inside and outside of the permeable layer. Constant and same slope is assumed for both layers with the constant discharge in the stream-wise direction. The depth of the seepage layer is assumed to be comparable with the flow depth in the river

flow layer. x' is considered as the stream-wise direction and the y' is considered the normal direction to the stream wise direction in a dimensional manner. Turbulent flow in rivers are formulated using the Navier-Stokes equations and the seepage flow is formulated by Brinkman-Forchheimer equations. Small perturbations are introduced on the normal flow condition and analysis is carried out to obtain the behavior of the perturbations with the time in terms of linear stability analysis.
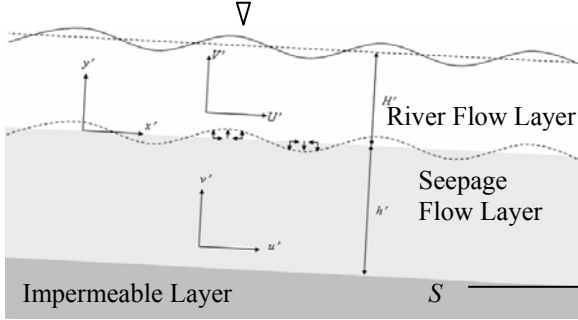
Fig. 1: The conceptual diagram of the model

3 Problem formulation

3.1 Governing equations for the river flow

River flow is formulated using the Navier-Stokes equations without time derivative terms. The time scale for the river flow is extremely small with the comparison of it in the seepage layer flow and it has been abolished from the governing equations. Non-dimensional governing equations are shown as

$$U\frac{\partial U}{\partial x}+V\frac{\partial U}{\partial y}=-\frac{\partial P}{\partial x}+\frac{\partial T_{xx}}{\partial x}+\frac{\partial T_{xy}}{\partial y}+1 \quad (1)$$

$$U\frac{\partial V}{\partial x}+V\frac{\partial V}{\partial y}=-\frac{\partial P}{\partial y}+\frac{\partial T_{yx}}{\partial x}+\frac{\partial T_{yy}}{\partial y}-\frac{1}{S} \quad (2)$$

$$\frac{\partial U}{\partial x}+\frac{\partial V}{\partial y}=0 \quad (3)$$

where x and y are the stream-wise and normal to the stream-wise direction respectively. U and V are the components of the velocity in the river flow in the x and y directions respectively, S, P and T_{ij} ($i, j = x, y$) are the average bed slope, the pressure and the Reynolds stress tensor respectively. The above equations have been non-dimensionalized by

$$(U',V')=U'_{fn}(U,V) \quad (4)$$

$$(x',y')=H'_{n}(x,y) \quad (5)$$

$$(P',T_{ij}')=\rho(U'_{fn})^{2}(P,T_{ij}) \quad (6)$$

$$v_{T}'=U'_{fn}H'_{n}(v_{T}) \quad (7)$$

$$(H',l',R')=H'_{n}(H,l,R) \quad (8)$$

$$U'_{fn}=\sqrt{gH'_{n}S} \quad (9)$$

where U'_{fn} and H'_{n} are the friction velocity and the flow depth in the base state flat bed condition. The Reynolds stress tensor is expressed by using the mixing length turbulent model which has been improved in the forms *(M. Colombini, 2004)*

$$(T_{xx},T_{yy})=2v_{T}(\frac{\partial U}{\partial x},\frac{\partial V}{\partial y}) \quad (10)$$

$$(T_{xy}=T_{yx})=v_{T}(\frac{\partial U}{\partial y}+\frac{\partial V}{\partial x}) \quad (11)$$

$$v_{T}=l^{2}\frac{\partial U}{\partial y} \quad (12)$$

$$l=\kappa(y+R)\sqrt{\frac{H-y}{H}} \quad (13)$$

where v_{T}, l, z, H and R are the eddy viscosity, mixing length, bed elevation, the flow depth and the reference level at which the velocity vanishes in the logarithmic velocity distribution respectively, and κ is the Karman constant which is 0.4 in this analysis.

3.2 Governing equations for the seepage flow

Seepage flow is expressed by the Brinkman-Forchheimer equations (*Derek B. Ingham and Iioan Pop 2002*) and the continuity equation in the non-dimensional form.

$$\frac{1}{\lambda}\frac{\partial u}{\partial t}+\frac{1}{\lambda^{2}}(u\frac{\partial u}{\partial x}+v\frac{\partial u}{\partial y})=-\frac{\partial p}{\partial x}+$$

$$\frac{\partial \tau_{xx}}{\partial x}+\frac{\partial \tau_{xy}}{\partial y}+1-\frac{\mu}{K}u-\frac{c_{F}}{\sqrt{K}}u\sqrt{u^{2}+v^{2}} \quad (14)$$

$$\frac{1}{\lambda}\frac{\partial v}{\partial t}+\frac{1}{\lambda^{2}}(u\frac{\partial v}{\partial x}+v\frac{\partial v}{\partial y})=-\frac{\partial p}{\partial y}+$$

$$\frac{\partial \tau_{yx}}{\partial x}+\frac{\partial \tau_{yy}}{\partial y}-\frac{1}{S}-\frac{\mu}{K}v-\frac{c_{F}}{\sqrt{K}}v\sqrt{u^{2}+v^{2}} \quad (15)$$

$$\frac{\partial u}{\partial x}+\frac{\partial v}{\partial y}=0 \quad (16)$$

where u and v are the components of the virtual velocity in the permeable layer in the x and y directions respectively, p, μ and λ are the pressure, the viscosity of water and the porosity respectively,

and τ_{ij} ($i, j = x, y$)which is the stress component of the seepage layer is expressed in the following form;

$$(\tau_{xx}, \tau_{yy}) = 2\frac{\mu}{\lambda}(\frac{\partial u}{\partial x}, \frac{\partial v}{\partial y}) \tag{17}$$

$$(\tau_{xy} = \tau_{yx}) = \frac{\mu}{\lambda}(\frac{\partial u}{\partial y} + \frac{\partial v}{\partial x}) \tag{18}$$

The above equations have been normalized by

$$(u', v') = U'_r(u, v) \tag{19}$$

$$(p', \tau_{ij}') = \rho U'_{fn}{}^2(p, \tau_{ij}) \tag{20}$$

$$\mu' = \rho U'_{fn} H'_n(\mu) \tag{21}$$

$$K' = H'_n{}^2(K) \tag{22}$$

$$\bar{t} = T_0 t \tag{23}$$

$$U'_r = \frac{\rho g S K'}{\mu'} \tag{24}$$

$$T_0 = \frac{U'_r}{\lambda g S} \tag{25}$$

where U'_r is sufficiently smaller than U'_{fn} and the time scale for the seepage flow, T_0 is sufficiently higher than the time scale of river flow.

3.3 Boundary and matching conditions
Tangential and normal stresses are vanished at the water surface ($y = H$). The kinematic boundary condition at the water surface is expressed as

$$V = \frac{\partial H}{\partial t} + U\frac{\partial H}{\partial x} \tag{26}$$

From the river flow layer to the seepage layer ($y = 0$) it has been assumed that the pressure and the tangential velocity are continuous, but shear stress is to be discontinuous. The following combination is obtained using the depth average continuity equation for the seepage layer.

$$h\frac{\partial \bar{u}}{\partial x} + v(0) = 0 \tag{27}$$

where $\bar{u}$ is the depth average velocity in the seepage layer for the x direction and it is assumed to be a constant along the depth of the seepage layer. Also the velocity in the depth direction is assumed to be

vanished and the shear stress is assumed to be neglected.

4 Base State Solution
4.1 Base state solution for river flow layer
The base state solution is obtained from the Navier Stokes equations without perturbations in the flat bed normal flow conditions. The governing equations are solved using boundary conditions to get the logarithmic velocity distribution in the river flow layer as

$$U = \frac{1}{\kappa}\ln(\frac{y + R}{R}) + \bar{u} \tag{28}$$

4.2 Base state solution for seepage flow layer
In the steady state, time and x derivative terms are dropped. From the Brinkman-Forchhimer equations, the depth-averaged velocity in the x direction is obtained as

$$\bar{u} = \frac{-\mu^2 + \sqrt{\mu^4 + 4\mu^2 c_F K^{3/2}}}{2c_F K^{3/2}} \tag{29}$$

5 Linear Stability Analysis
Stream function is introduced to the river flow and variables are expanded in the forms

$$(U, V) = \left(\frac{\partial \psi}{\partial y}, -\frac{\partial \psi}{\partial x}\right) \tag{30}$$

$$(\psi, P, H, \bar{u}) = (\psi_0, P_0, 1, \bar{u}_0) +$$
$$A(\widetilde{\psi}_1, \widetilde{P}_1, \widetilde{H}_1, \widetilde{\bar{u}}_1) \tag{31}$$

$$(\widetilde{\psi}_1, \widetilde{P}_1, \widetilde{H}_1, \widetilde{\bar{u}}_1) =$$
$$\left[\psi_1(y), P_1(y), H_1(y), \bar{u}_1\right]e^{i(kx - \omega t)} \tag{32}$$

where A is the amplitude of the perturbation, which is an infinitesimally small, k and ω are the wave number and the complex angular frequency of the perturbation, respectively. Governing equations are solved mathematically using the Chebyshev polynomials. Porosity is considered to be 0.6 for the analysis.

6 Results
It has been understood that the particle diameter of the sediments and the longitudinal slope of the river

and seepage layer are the two most important factors to the hyporheic interaction (*Daniele Tonina et al 2007 and Andrew J. Boulton et al 1998)*. Therefore the analysis was carried out for two slopes of the combined river flow and seepage flow layers as 0.001 and 0.01. Also the growth rate contours are plotted in the dimensionless particle diameter (Dp) and wave number (k) axes system. Fig. 2 and Fig. 3 show the imaginary part of the growth rate of perturbation as a function of dimensionless particle diameter and the wave number when the slopes are 0.001 and 0.01 respectively. These instability diagrams were obtained at the small wave numbers.

$$D_p = \frac{d}{H'_n} \tag{33}$$

where d is the particle diameter. In order to address the real situation, the particle diameter should be small enough with the height of the river flow layer. Therefore the considered dimensionless particle diameter was decreased. The particle diameter is considered to be one tenth of the river water depth as the maximum. Fig. 4 and Fig. 5 are the magnified figures along the dimensionless particle diameter axis.
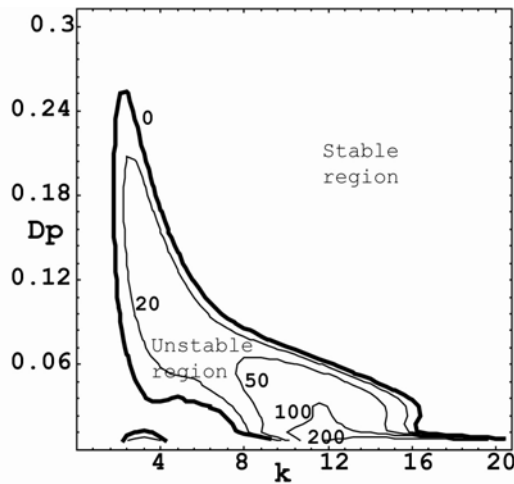
Fig. 2: The imaginary part of the growth rate contours of the perturbations for S = 0.001 with small wavenumbers
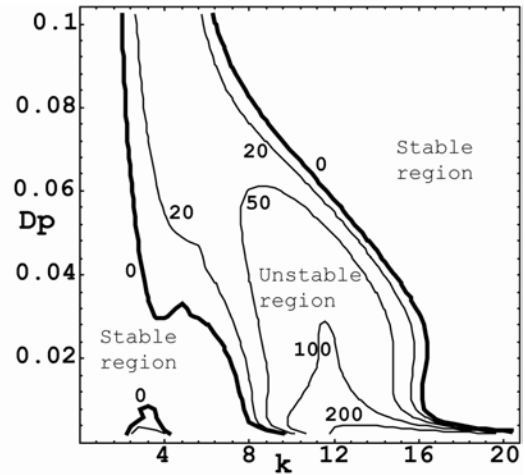
Fig. 4: The magnified imaginary part of the growth rate contours of the perturbations S = 0.001 with small wavenumbers
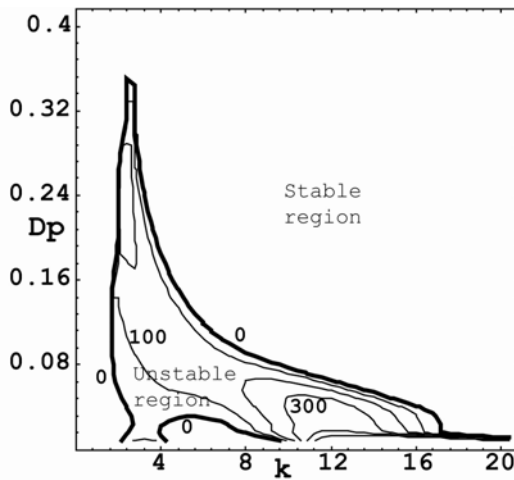
Fig. 3: The imaginary part of the growth rate contours of the perturbations for S = 0.01 with small wavenumbers
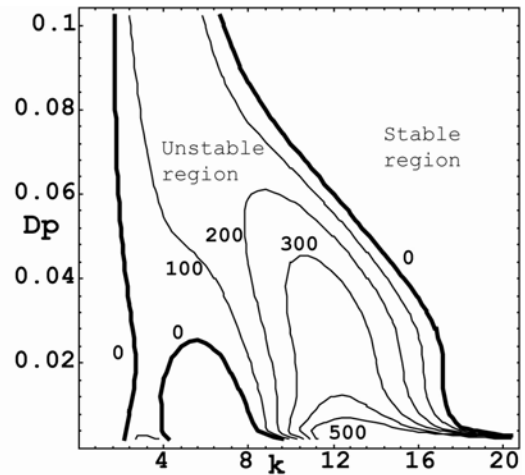
Fig. 5: The magnified imaginary part of the growth rate contours of the perturbations S = 0.01 with small wavenumbers

The dimensionless particle diameter was non-dimensionalized by

Fig. 6 and Fig. 7 show the real part of the growth rate contours of the perturbations in the small wave numbers when the slopes are 0.001 and 0.01

respectively. The phase velocities of the waves are denoted by these contour lines in the dimensionless particle diameter and wavenumber axes system.
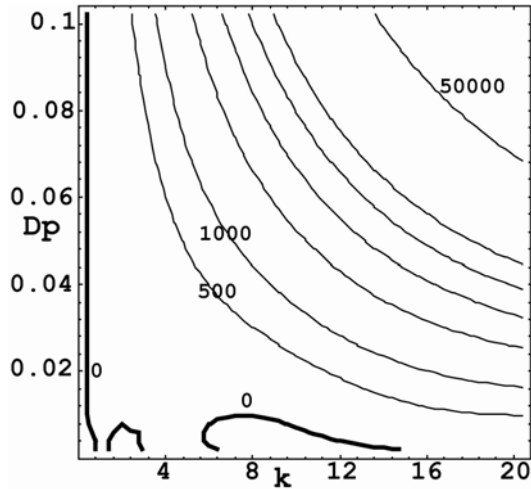
Fig. 6: The real part of the growth rate contours of the perturbations for S = 0.001 with small wavenumbers
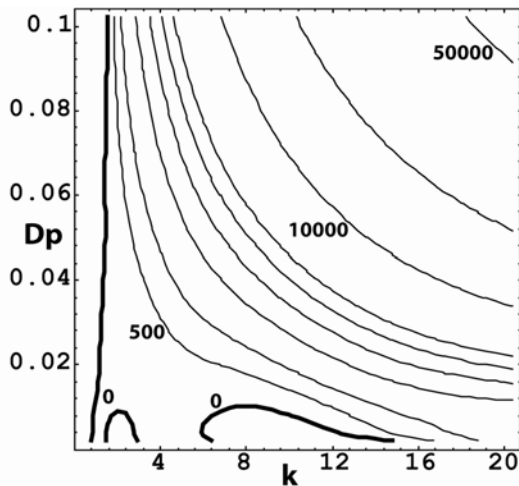
Fig. 7: The real part of the growth rate contours of the perturbations for S = 0.01 with small wavenumbers

Another instability region is found when the wavenumbers are in the range of 40 to 100 and the imaginary part of the growth rate contours of the perturbations are shown at 0.001 and 0.01 slopes respectively by Figs. 8 and 9.

Figs. 10 and 11 are the real part of the growth rate contours of the perturbations and these denote the phase velocities of the waves as discussed above for Figs. 6 and 7.
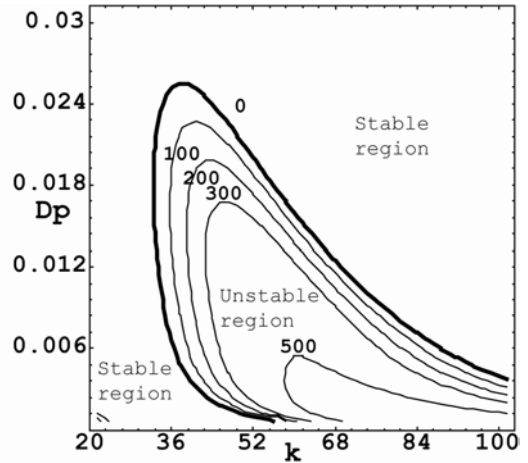
Fig. 8: The imaginary part of the growth rate contours of the perturbations for S = 0.001 with large wavenumbers
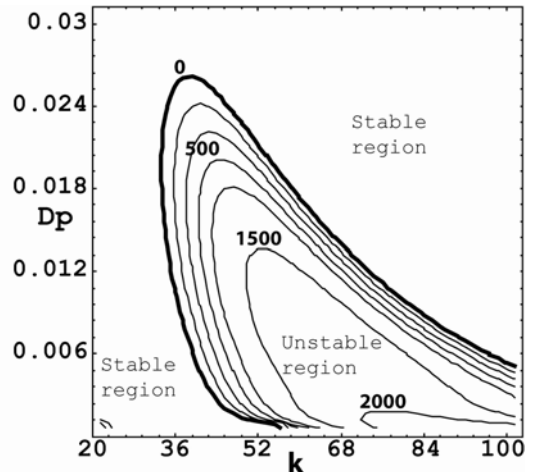
Fig. 9: The imaginary part of the growth rate contours of the perturbations for S = 0.01 with large wavenumbers
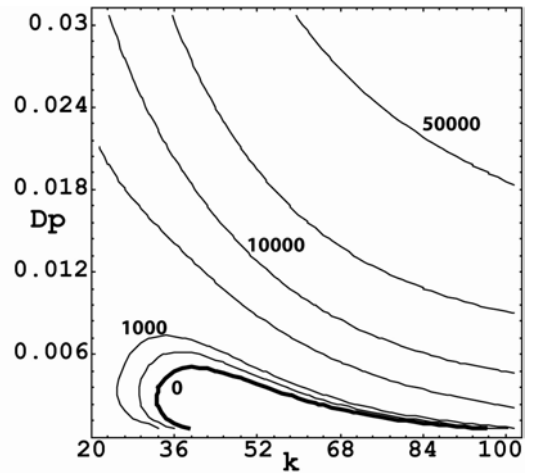
Fig. 10: The real part of the growth rate contours of the perturbations for S = 0.01 with large wavenumbers
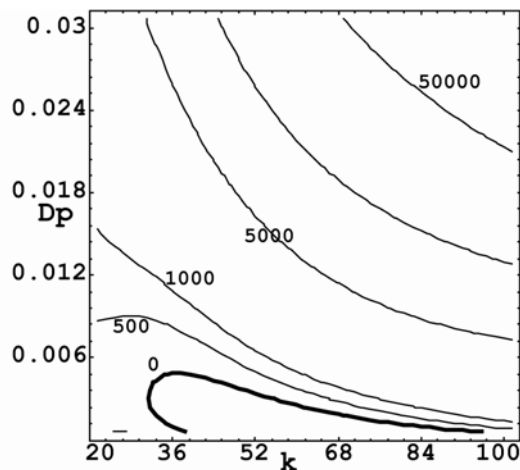
Fig. 11: The real part of the growth rate contours of the perturbations for S = 0.001 with large wave numbers

7 Conclusions

The thick black lines of Figs. 2 - 9 show the neutral curve where the growth rate of is zero. Inside the neutral curve growth rate is positive, which means that the growth rate of the perturbation that we have introduced increases. Therefore it can be concluded that the normal flow is unstable. This means that the instability occurs among the river flow and seepage layers inside the neutral curve at the shown wave numbers and the dimensionless particle diameters.

Outside the neutral curve the growth rate is negative which means that the growth rate of the small perturbation decreases. Therefore it can be concluded that the normal flow is stable and instability is not occurred the outside of the neutral curve.

It is important to recognize another instability region when the wave numbers are comparably high as shown in Figs. 8 and 9. This means that the wave lengths are quite small and interaction occurs with the small wavelengths. Even though it is quite strange the theoretical results should be further understood through an experimental study.

By comparison of the Figs. 4 and 5 it has been noted that the range for the occurrence of instability region increases with the slope. However this interesting process cannot be understood from the Figs. 8 and 9. Therefore, it can be concluded that the interaction is improved with the slope when the wave numbers are small enough.

It is understood that the phase velocities of waves are increased with the dimensionless particle diameter rapidly from the Figs. 6, 7, 10 and 11. Therefore the experimental studies should be carried out in the small number of dimensionless particle diameters.

References:
[1] Andrew J. Boulton, Stuart Findlay, Pierre Marmonier, Emily H. Stanley and H. Maurice Valett, The Functional Significance of the Hyporheic Zone in Streams and Rivers, *Annual Review of Ecology and Systematic*, 29, 1998, pp. 59-81.
[2] Daniele Tonina and M. Buffington, Hyporheic Exchange in Gravel Bed Rivers with Pool-riffle Morphology; Laboratory Experiments and Three Dimensional Modeling, *Water Resources Research*, VOL 43, 2007
[3] Andrea Butturini, Susana Bernal, Sergi Sabater and Francesc Sabater, The influence of riparian-hyporheic zone on the hydrological responses in an intermittent stream, *Hydrology and Earth System Sciences,* 6(3), 2002, pp. 515-525.
[4] Kenneth E. Bencala, Hyporheic Zone Hydrological Processes, *Hydrological Processes Today,* VOL 14, 2000, pp.2797-2798.
[5] *Colombini M. (2004). Revisiting the Linear Theory of Sand Dune Formation.* Journal of Fluid Mechanics, 502, 1-16
[6] Derek B. Ingham and Iioan Pop, Transport Phenomena in Pporous Media II, 1st Edition, Elsevier Science Ltd. ISBN: 0-08-043965-9, 2002.